Polyhedron 228 (2022) 116162

Contents lists available at ScienceDirect

Polyhedron

journal homepage: www.elsevier.com/locate/poly

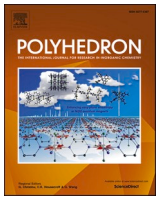

Synthesis and crystal structure of an iridium complex containing the novel electron-poor hybrid monoanionic ligand $Ph_2PCF_2PO_2(OiPr)$☆

Daniel J. Sattler [a], Jake B. Bailey [b], Douglas B. Grotjahn [a,*]

[a] Department of Chemistry, San Diego State University, San Diego, CA 92182, United States
[b] Department of Chemistry and Biochemistry, University of California San Diego, La Jolla, CA 92093, United States

ARTICLE INFO

Keywords:
Electron poor
Iridium
Bidentate ligand
Bifunctional ligand
Phosphonate

ABSTRACT

Phosphines have long been used in catalysis, and a wide variety of ligands with almost any substituent are available. However, the vast majority of these phosphines have been relatively electron-rich. Monooxides of bisphosphines have been shown to form complexes that catalyze alkene polymerizations and hydroformylations. However, electron-poor versions of such ligands have not yet been explored. In this report, the hybrid ligand $Ph_2PCF_2PO_2(O^iPr)$ with both phosphine and phosphonate ester moieties, linked with an electron deficient CF_2 group was synthesized. A Cp*Ir complex of the ligand was synthesized and characterized.

1. Introduction

Phosphines have long been used in catalysis, and a wide variety of ligands with almost any substituent are available. However, the vast majority of these phosphines are relatively electron-rich. A significant amount of research has also been devoted to the organic transformation of alkenes into other functional groups. Monooxides of bisphosphines (BPMO, **A** in Chart 1) have been shown to form complexes that catalyze alkene polymerizations [1–3] and hydroformylations [4]. However, more electron-poor ligands of type **A** have been unexplored so far. The goal of this project was to synthesize a hybrid P,O-ligand of type **D** in Chart 1 which is electron-poor, and then modify the electronic and steric properties of this class of ligand further and to include pendant base or acid functionality as part of the ligand.

Electron-poor ligands have been underexplored in the literature. Several studies have shown how they can affect the reductive elimination step of a catalytic cycle, even to the point of outcompeting β-hydride elimination [5]. They have also been used to examine how effective they are in previously studied chemistry such as cross-coupling, hydroformylation [6] and carbonylation [7]. Several studies describe the properties and suitability of electron-poor ligands for catalysis [8,9], and several more discuss their use in stoichiometric reactions [10–12]. Reviews that focus on electron-poor phosphines discuss synthesis of the ligands and related metal complexes, but reactivity studies were limited to polymerization and hydrogenation [13].

The Grotjahn group has focused on the usage of ligands containing a pendant base, finding them to have a significant impact on the rate [14] and selectivity [15] of a reaction. Combining electron-poor and bifunctional ligands would give a new type of ligand with unexplored properties. Another attractive feature of a bifunctional ligand is its ability to coordinate in a chelating manner, which utilizes the chelate effect to help the ligand stay coordinated [16], a concern when using electron-poor ligands.

In this work, a bifunctional, electron-poor ligand of type **D** and an associated Ir complex were synthesized and characterized. While no new reactivity was discovered from the complex, the ligand and complex by themselves and their syntheses are novel and hence are reported here.

2. Materials and methods

Nuclear magnetic spectra were recorded on a Varian VNMRS 400 MHz spectrometer with AutoX probe. Deuterated methanol and deuterated chloroform were stored over 3 and 4 Å molecular sieves, respectively. Signals were referenced to $SiMe_4$ through the residual solvent resonance. Diethyl ether was distilled from sodium and benzophenone. Dichloromethane was distilled from calcium hydride. Toluene was degassed, and all organic solvents were stored in a glove box under nitrogen over 4 Å molecular sieves. Water was degassed and stored under nitrogen in a glove box. Chlorodiphenylphosphine and *t*-butyl lithium (1.9 M in pentane) were purchased from Sigma Aldrich and used without further purification. Diisopropyl (difluromethyl)phosphonate (**1**) was synthesized according to literature procedure. Elemental

☆ This paper is dedicated to Professor Arnie Rheingold for his devotion to x-ray crystallography and his peerless friendship over the years.
* Corresponding author.

https://doi.org/10.1016/j.poly.2022.116162
Received 5 May 2022; Accepted 1 October 2022
Available online 6 October 2022

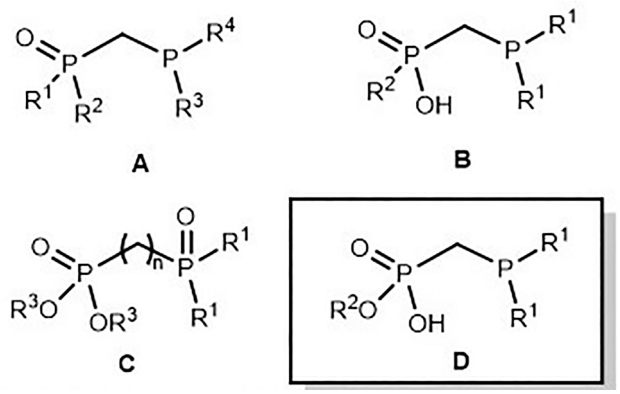

Chart 1. Comparison of similar bisphosphines ligands and this work.

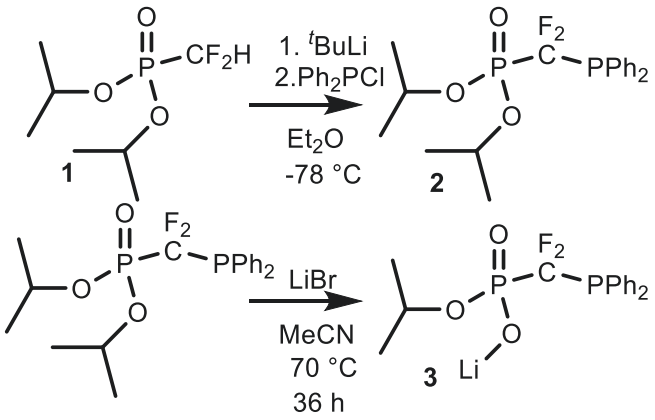

Scheme 1. Synthesis of **3.**

analysis was performed by NuMega Resonance labs in San Diego, CA. Coupling constants are reported in Hz.

Synthesis of **2**: Diisopropyl (difluoromethyl)phosphonate (**1**) (2.699 g, 12.5 mmol) and THF (120 mL) were added to a Schlenk flask, which was cooled to −78 °C. *tert*-butyl lithium (6.8 mL, 1.9 M/L in pentane) was added dropwise over 5 min, and the reaction was stirred for 1 h. Chlorodiphenylphosphine (2.756 g, 12.5 mmol) was added dropwise, and the reaction was allowed to warm to ambient temperature over 4 h. The volatiles were then removed under vacuum. The residue was dissolved in DCM (25 mL) and washed with water (3 × 50 mL). The organic layer was collected and the volatiles removed under vacuum to give 3.333 g (66 %) of the crude product. This was used without further purification.

$^{31}P\{^{1}H\}$ ($CDCl_3$): δ 26.1 (p, $J_{P\text{-}F}$ 26.3). ^{19}F ($CDCl_3$) δ −109.0 (dd, $J_{P\text{-}F}$ 70, 95). ^{1}H ($CDCl_3$): 7.70 (t, $J_{H\text{-}H}$ 8, 4H), 7.40 (m, 6H), 4.75 (h, $J_{H\text{-}H}$ 6, 2H), 1.25 (dd, $J_{P\text{-}H}$ 22, $J_{H\text{-}H}$ 6, 12H).

Synthesis of **3: 2** (1.00 g, 2.5 mmol), acetonitrile (0.50 mL), and LiBr (0.217 g, 2.5 mmol) were added to a scintillation vial equipped with a stir bar. The reaction was heated at 70 °C for 18 h, removed from the heat and shaken, and then heated for another 18 h. The mixture was then cooled to room temperature, filtered, and the precipitate was washed with acetonitrile (1 × 5 mL), DCM (1 × 5 mL), and diethyl ether (1 × 5 mL). The white powder was then dried overnight under vacuum giving 0.910 g (58 %) of product.

$^{31}P\{^{1}H\}$ (MeOD): δ 3.2 (td, $J_{P\text{-}F}$ 82), 1.1 (q, $J_{P\text{-}F} = J_{P\text{-}P}$ 60). ^{1}H (MeOD): δ 7.65 (td, $J_{H\text{-}H}$ 7.5, 2, 4H), 7.45–7.35 (m, 6H), 4.52 (h, $J_{H\text{-}H}$ 6, 1H), 1.12 (d, $J_{H\text{-}H}$ 6, 6H). ^{13}C (MeOD): δ 135.0 (d, $J_{P\text{-}C}$ 20), 132.8 (dtd, $^{1}J_{P\text{-}C}$ 13.2, $^{3}J_{P\text{-}F}$ 4.5, $^{3}J_{P\text{-}C}$ 2.2, assigned to ipso carbon of Ph), 128.9 (s), 127.6 (d, $J_{P\text{-}C}$ 7.6), 69.8 (dd, $J_{P\text{-}C}$ 6.8, 6.4), 23.5 (d, $J_{P\text{-}C}$ 4.1); signal for CF_2 carbon is expected to be a dtd, and some of the signal resonances are seen but others are obscured by much more intense signals. Negative ion mode QTOF-MS *m/z* for $C_{16}H_{17}F_2O_3P_2$: Calculated 357.06211; Obtained 357.0675.

Synthesis of **4**: ligand **3** (0.100 g, 0.274 mmol) was added to a scintillation vial equipped with a stir bar. $[IrCp^*Cl_2]_2$ (0.1093 g, 0.137 mmol) was then added, and 1.3 mL of CH_2Cl_2 was added. The reaction was stirred overnight, and the solvent was removed to give 0.1989 g of residue. To the mixture was added 5 mL of CH_2Cl_2, which was filtered and the filtrate concentrated to give **4** (0.098 g, 45 % yield). X-ray quality crystals were grown by the slow evaporation of CH_2Cl_2 from a

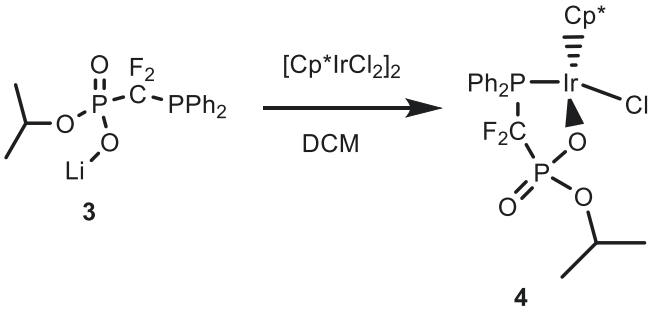

Scheme 2. Synthesis of **4.**

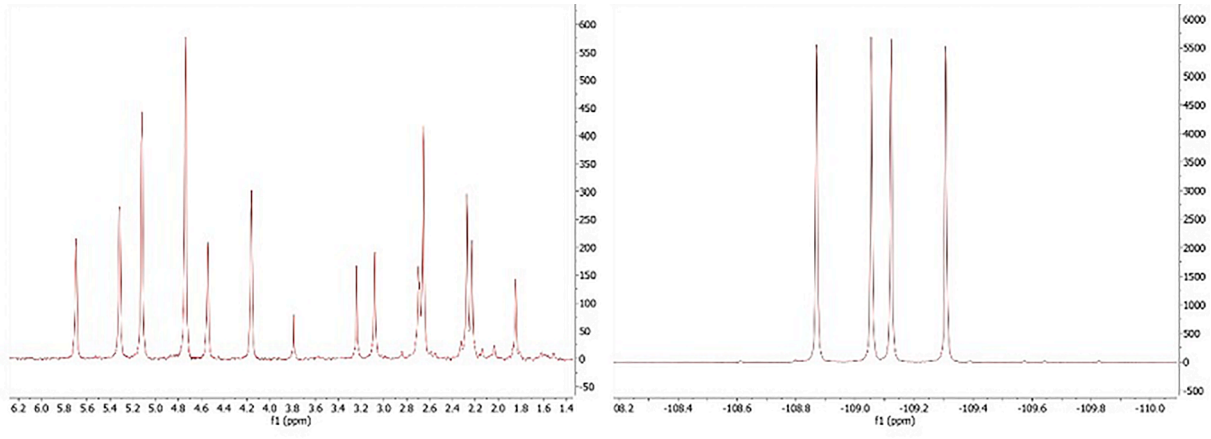

^{31}P NMR Spectrum of 2 ^{19}F NMR Spectrum of 2

Fig. 1. Left and right, respectively, ^{31}P and ^{19}F NMR spectra of **2** in $CDCl_3$ at 161 and 376 MHz.

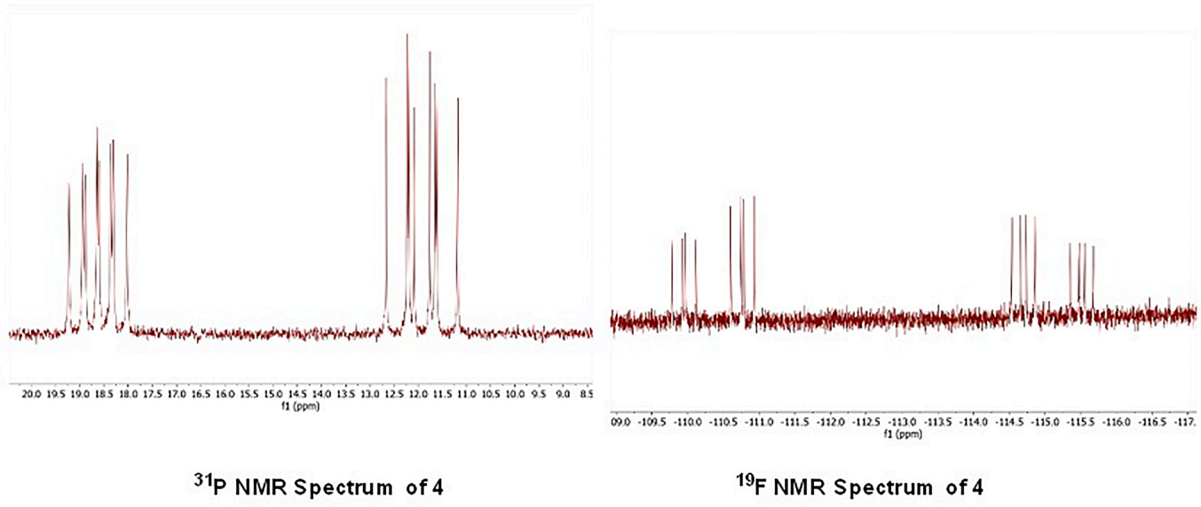

Fig. 2. Left and right, respectively, ^{31}P and ^{19}F NMR spectra of **2** in $CDCl_3$ at 161 and 376 MHz respectively.

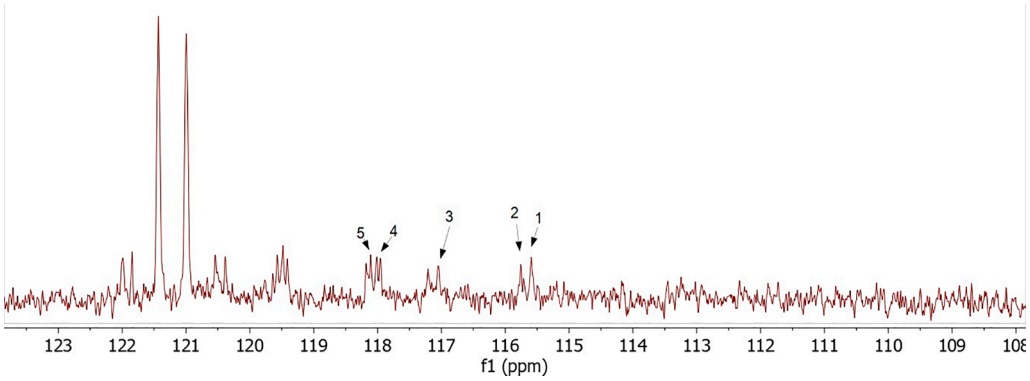

Fig. 3. Inset of ^{13}C NMR spectrum of **4** highlighting the 16-peak dddd for the CF_2 carbon. Frequencies for the peaks 1 to 5 are: 14531.0, 14552.0, 14715.0, 14828.4, 14847.6 Hz, respectively, giving *J* values of 21.0, 184.0, 297.3, and 316.6 Hz.

saturated solution of **4**. $^{31}P\{^1H\}$ ($CDCl_3$): δ 19.6 (td, $J_{P\text{-}P}$ 92, $J_{P\text{-}F}$ 44, 54), 11.5 (dt, $J_{P\text{-}P}$ 92, $J_{P\text{-}F}$ 74). ^{13}C ($CDCl_3$): δ 136.2 (d, $J_{P\text{-}C}$ 11.0), 134.3 (d, $J_{P\text{-}C}$ 10.0), 132.3, 131.9, 128.6 (d, $J_{P\text{-}C}$ 11.3), 128.5 (sl br d, $J_{P\text{-}C}$ 11.0), 127.5 (d, $J_{P\text{-}C}$ 58.4), 121.2 (d, $J_{P\text{-}C}$ 53.3), 118.8 (dddd, $J_{F\text{-}C}$ 316.6, 297.3, $J_{P\text{-}C}$ 184.0, 21.0), 93.1 (d, $J_{P\text{-}C}$ 2.8), 73.23 (d, $J_{P\text{-}C}$ 5.7), 73.18 (d, $J_{P\text{-}C}$ 5.7), 24.4 (d, $J_{P\text{-}C}$ 3.0), 24.0 (d, $J_{P\text{-}C}$ 5.0), 8.6. ^1H ($CDCl_3$) 7.75 (t, 11.3, 2H), 7.58 (t, 9.2, 1H), 7.50 (t, 6.0, 1.5H), 7.45 (s, 2H), 4.76 (h, 4.9, 1H), 1.48 (s, 15H), 1.28 (d, $J_{H\text{-}H}$ 5.6, 6H). Elem. anal. calcd for $C_{26}H_{32}ClF_2IrO_3P_2$ (720.14): C, 43.36; H, 4.48. Found: C, 39.84; H, 4.54. Elem. anal. calcd for $C_{26}H_{32}ClF_2IrO_3P_2 + 3.5\ H_2O$ (783.20): C, 39.87; H, 5.02.

3. Results and discussion

The present investigation began with the design of a model compound that could be used to determine the most efficient method of synthesizing hybrid ligands of type **D** (see Chart 1) using **A** as a starting point. A diphenylphosphino substituent was chosen for the initial synthesis, but the substituents on the phosphine portion of the ligand could readily be changed to make it more electron-poor once the initial synthesis was optimized. The anion of **1** (Scheme 1) has been used in a variety of syntheses [17–20], and **1** was readily available in one step [21].

The synthesis of **2** initially seemed quite straightforward (Scheme 1), with the addition of *t*-butyl lithium to **1** at −78 °C, followed by addition of chlorodiphenylphosphine. The initial purification with a water wash to remove lithium followed by removal of volatile compounds *in vacuo* gave a crude clear, viscous liquid. The crude yield was 80 %, and NMR spectroscopy showed mostly (ca. 90 %) one compound. Due to the number of NMR active nuclei in compound **2**, the spectra were complicated (Fig. 1), but this also allowed a more certain identification. In the ^{31}P NMR spectrum shown below, two partly overlapping signals were seen at 4.90 and 2.59 ppm, with $^2J_{P\text{-}P}$ = 62.1 Hz, as well as coupling to the two fluorine atoms $^2J_{P\text{-}F}$ = 93.1 and 69.0 Hz, respectively. The ^{19}F NMR spectrum showed a corresponding doublet of doublets, $^2J_{F\text{-}P}$ = 93.1 Hz, $^2J_{F\text{-}P}$ = 69.0 Hz.

Although the identity of **2** is assured, purification was much less straightforward. Compound **2** was found to be quite capable of coordinating Li ions formed from the *t*-butyl lithium used in the initial synthesis, verified by ^7Li NMR spectroscopy. While the lithium was easily removed using a water wash, **2** decomposed upon attempted distillation even under reduced pressure, and column chromatography led to very poor mass recovery (less than5%). It was suspected that **2** decomposed through a radical pathway, in part because both Ph_2P [22] and fluoroalkyl radicals are known species [23–25].

To move past these issues, impure **2** was used in subsequent reactions. Several methods of phosphonate diester hydrolysis were attempted. Refluxing **1** with NaOH in water or Me_3SiBr in dichloromethane led to a mixture of several products. Gratifyingly, refluxing **1** with LiBr in dry acetonitrile [26] lead to crystalline product **3** in 58 % yield, pure enough for metallations (Scheme 2).

The initial target was an IrCp* complex, which was synthesized by stirring $[IrCp^*Cl_2]_2$ and **3** in dichloromethane overnight to give the metal complex in 95 % yield (Scheme 2). The ^{31}P NMR spectrum (Fig. 2)

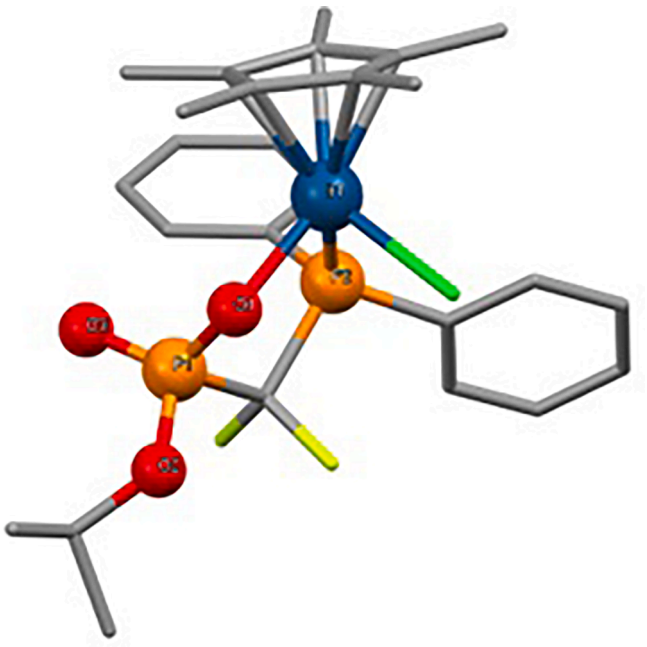

Fig. 4. Ball and stick representation of the molecular structure of **4** as determined by X-ray diffraction. The Ir, P, and O atoms are highlighted by representing them as spheres, whereas all other nonhydrogen atoms are represented using sticks. Key bond distances (Å): Ir-P 2.295, Ir-O 2.149, Ir-Cl 2.385. Key angles: O-Ir-P 87.06°, O-Ir-Cl 83.05°, and Cl-Ir-P 91.36°.

showed two signals, each a ddd, with *J* values matching those for the two signals in the ^{19}F NMR spectrum, consistent with mutual coupling. Combined, these data indicate the presence of only one diastereomer.

Interestingly, the ^{13}C NMR spectrum of **4** indicated that all carbons of the ligand were unique, consistent with the two phenyls being diastereotopic, and also the two isopropyl methyls. Moreover, the CF_2 carbon appeared as a remarkable 16-line dddd pattern, barely resolved even after overnight acquisition (Fig. 3). The two largest splittings (316.6 and 297.3 Hz) were similar and were assigned to $^{1}J_{F\text{-}C}$, where the 21.0 Hz splitting was ascribed to $^{1}J_{PPh2\text{-}C}$ and the 184.0 Hz one to $^{1}J_{PO2(OiPr)\text{-}C}$ [27]. While no water was seen in the proton NMR spectrum for **4**, the elemental analysis was consistent with the presence of 3.5 water molecules per complex. As the complex is air stable, no precautions were taken in the lab or the lab of the company that performed the analysis to exclude water from the sample.

X-ray quality crystals of **4** were grown by slow evaporation of dichloromethane (Fig. 4). The Ir-O3 bond distance in **4** was 2.149 Å, compared to 2.150 Å for the similar complex κ-*O,P*- ($Ph_2PC_6H_4PO_3H$) Cp*ClIr)) [28]. The Ir-Cl bond length of 2.408 is also similar to the Ir-Cl bond in **4** of 2.385 Å [28].

In order to understand why only one isomer was seen in the NMR spectra and crystal structure, DFT calculations were performed to determine if there were structural differences preventing the formation of more than one isomer. Gas phase calculations were carried out using b3lyp/SDD as the functional and basis set, respectively. The observed diastereomer with isopropyl cis to chloride was found to be more stable than the trans diastereomer by 1.1 kcal/mol, and when dispersion was included in the calculations this difference increased to 3.4 kcal/mol between the two isomers, giving a K_{eq} of 295 at room temperature, corresponding to less than 0.1 % of the less stable trans isomer, which explained why both the NMR spectra and the isolated crystal showed evidence of only one species, that is also the complex calculated to be more stable. Both diastereomers are shown for comparison (Fig. 5).

However, examination of the structural features of the two different isomers did not give a clear reason why the observed isomer is preferred; a combination of subtle electronic and structural factors might contribute to this energy difference [29].

In order to test the metal complex for catalytic activity, **3** was ionized using silver hexafluorophosphate, and the resulting mixture was filtered through a silica plug into a J. Young NMR tube, and then hexene and either acetic acid or water was added. Tetrakis(trimethylsilyl)methane was used as an internal standard. The solution was monitored for changes over several days and then heated to 70 °C for 12 h but no changes were seen. No addition to the alkene was seen with either acetic acid or with water. A small amount of isomerization was seen, but Cp*Ir complexes are known to isomerize alkenes and there are already several good methods to isomerize alkenes [30].

4. Conclusions

A new chelating electron-poor ligand was synthesized, and its ability to coordinate to a metal was demonstrated. The resulting complex formed as a single diastereomer, and DFT calculations support a significant free energy difference between diastereomers. While the resulting complex was inactive as an alkene isomerization catalyst, the fact that no hybrid ligand containing both a phosphine moiety as well as a phosphonate moiety is known and the fact that there appears to be only one Cp*Ir-BPMO complex known all motivate this report.

Declaration of Competing Interest

The authors declare that they have no known competing financial

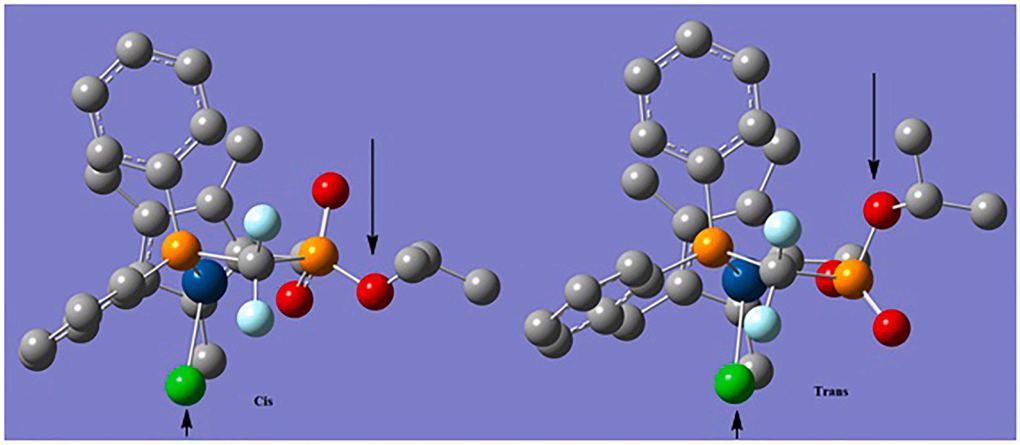

Fig. 5. Ball and stick representations of the calculated molecular structures showing cis and trans isomers, trans being lower energy. The arrows point to the green Cl atom and the O of the O-iPr group.

interests or personal relationships that could have appeared to influence the work reported in this paper.

Data availability

Data will be made available on request.

Acknowledgements

This work is financially supported by the NSF, grant CHE-2102623. We would like to thank Dr. Gregory Elliott for high-accuracy mass spectrometry services, and Dr. David Onofrei for NMR spectroscopy assistance.

Appendix A. Supplementary data

Supplementary data to this article can be found online at https://doi.org/10.1016/j.poly.2022.116162.

References

[1] K. Li, J. Ye, Z. Wang, H. Mu, Z. Jian, Indole-bridged bisphosphine-monoxide palladium catalysts for ethylene polymerization and copolymerization with polar monomers, Polymer Chemistry 11 (2020) 2740–2748.
[2] J. Jung, H. Yasuda, K. Nozaki, Copolymerization of Nonpolar Olefins and Allyl Acetate Using Nickel Catalysts Bearing a Methylene-Bridged Bisphosphine Monoxide Ligand, Macromolecules 53 (2020) 2547–2556.
[3] A. Hamada, P. Braunstein, Lithium−Palladium Complex Supported by Phosphonatophosphine and Chloride Ligands, Inorg. Chem. 47 (2008) 3934–3936.
[4] I. Le Gall, P. Laurent, E. Soulier, J.-Y. Salaün, H. des Abbayes, Complexation on rhodium of bidentate and potentially hemilabile phosphorous ligands, J. Organomet. Chem. 567 (1998) 13–20.
[5] R. Wursche, T. Debaerdemaeker, M. Klinga, B. Rieger, Electron-Poor Olefin Polymerization Catalysts Based on Semi-Fluorinated Bis(phosphane)s, Eur. J. Inorg. Chem. 2000 (2000) 2063–2070.
[6] M.L. Clarke, D. Ellis, K.L. Mason, A.G. Orpen, P.G. Pringle, R.L. Wingad, D. A. Zaher, R.T. Baker, The electron-poor phosphines P{$C_6H_3(CF_3)_2$–3,5}$_3$ and P(C_6F_5)$_3$ do not mimic phosphites as ligands for hydroformylation. A comparison of the coordination chemistry of P{$C_6H_3(CF_3)_2$–3,5}$_3$ and P(C_6F_5)$_3$ and the unexpectedly low hydroformylation activity of their rhodium complexes, Dalton Trans (2005) 1294–1300.
[7] A.M. Trzeciak, H. Bartosz-Bechowski, Z. Ciunik, K. Niesyty, J.J. Ziólkowski, Structural studies of $PdCl_2L_2$ complexes with fluorinated phosphines, phosphites, and phosphinites as precursors of benzyl bromide carbonylation catalysts, and and X-ray crystal structure of cis -$PdCl_2$ [PPh_2(OEt)]$_2$, Can. J. Chem. 79 (2001) 752–759.
[8] S. Hussein, D. Priester, P. Beet, J. Cottom, S.J. Hart, T. James, R.J. Thatcher, A. C. Whitwood, J.M. Slattery, Filling a Niche in “Ligand Space” with Bulky, Electron-Poor Phosphorus(III) Alkoxides, Chem. Eur. J. 25 (2019) 2262–2271.
[9] B.G. Anderson, J.L. Spencer, The Coordination Chemistry of Pentafluorophenylphosphino Pincer Ligands to Platinum and Palladium, Chem. Eur. J. 20 (2014) 6421–6432.
[10] V. Alezra, G. Bernardinelli, C. Corminboeuf, U. Frey, E.P. Kündig, A.E. Merbach, C. M. Saudan, F. Viton, J. Weber, [CpRu((R)-Binop-F)(H_2O)][SbF_6], a New Fluxional Chiral Lewis Acid Catalyst: Synthesis, Dynamic NMR, Asymmetric Catalysis, and Theoretical Studies, J. Am. Chem. Soc. 126 (2004) 4843–4853.
[11] M.E. Bruin, E. Peter Kündig, A new chiral ligand for the Fe–Lewis acid catalysed asymmetric Diels-Alder reaction, Chem. Commun. (1998) 2635–2636.
[12] S. Thamapipol, B. Ludwig, C. Besnard, C. Saudan, E.P. Kündig, Ruthenium Lewis Acid-Catalyzed Asymmetric Diels-Alder Reactions: Reverse-Face Selectivity for α, β -Unsaturated Aldehydes and Ketones, Helv. Chim. Acta 99 (2016) 774–789.
[13] A.K. Brisdon, C.J. Herbert, Fluoroalkyl-containing phosphines, Coord. Chem. Rev. 257 (2013) 880–901.
[14] D.B. Grotjahn, D.A. Lev, A General Bifunctional Catalyst for the Anti-Markovnikov Hydration of Terminal Alkynes to Aldehydes Gives Enzyme-Like Rate and Selectivity Enhancements, J. Am. Chem. Soc. 126 (2004) 12232–12233.
[15] C.R. Larsen, G. Erdogan, D.B. Grotjahn, General catalyst control of the monoisomerization of 1-alkenes to trans-2-alkenes, J. Am. Chem. Soc. 136 (2014) 1226–1229.
[16] 7 - Enthalpy-Driven Reactions I: Acid–Base Reactions, in: W.W. Porterfield (Ed.) Inorganic Chemistry (Second Edition), Academic Press, San Diego, 1993, pp. 361-406.
[17] Y. Yamamoto, Y. Ishida, T. Kurohara, M. Shibuya, T. Yasui, Synthesis of γ-Difluoromethylated Tetronate Derivatives from Squarates Using Difluoromethylphosphonate, Heterocycles 99 (1) (2019) 363.
[18] C. Alter, B. Hoge, Synthesis and characterization of a novel difluoromethylene phosphonic acid functionalized polymer, J. Appl. Polym. Sci. 135 (42) (2018) 46765.
[19] C. Cocaud, C. Nicolas, T. Poisson, X. Pannecoucke, C.Y. Legault, O.R. Martin, Tunable Approach for the Stereoselective Synthesis of 1-C-Diethylphosphono (difluoromethyl) Iminosugars as Glycosyl Phosphate Mimics, J. Org. Chem. 82 (2017) 2753–2763.
[20] Z. Feng, F. Chen, X. Zhang, Copper Catalyzed Cross-Coupling of Iodobenzoates with Bromozinc-difluorophosphonate, Org. Lett. 14 (2012) 1938–1941.
[21] G.M. Blackburn, G. Hägele, A. Hottgenroth, A.J. Ivory, D.L. Jakeman, R. Spiske, Automated lineshape analysis of complex NMR spectra for a novel synthetic tetrafluorobisphosphonate, a potential ligand for phosphoglycerate kinase, Phosphorus, Sulfur, Silicon Rel. Elem. 191 (3) (2016) 367–372.
[22] T. Lequeux, F. Lebouc, C. Lopin, H. Yang, G. Gouhier, S.R. Piettre, Sulfanyl- and Selanyldifluoromethylphosphonates as a Source of Phosphonodifluoromethyl Radicals and Their Addition onto Alkenes, Org. Lett. 3 (2) (2001) 185–188.
[23] Y. Chernykh, P. Beier, Development of (2-bromo-1,1,2,2-tetrafluoroethyl)(phenyl) sulfane as tetrafluoroethyl-radical and tetrafluoroethylene-diradical synthons for additions to alkenes, J. Fluorine Chem. 156 (2013) 307–313.
[24] S. Barata-Vallejo, M.V. Cooke, A.l. Postigo, Radical Fluoroalkylation Reactions, ACS Catal. 8 (8) (2018) 7287–7307.
[25] C.P. Zhang, Q.Y. Chen, Y. Guo, J.C. Xiao, Y.C. Gu, Progress in fluoroalkylation of organic compounds via sulfinatodehalogenation initiation system, Chem. Soc. Rev. 41 (2012) 4536–4559.
[26] J.M. Smith, R.J. Vierling, C.F. Meyers, Selective inhibition of E. coli1-deoxy-d-xylulose-5-phosphate synthase by acetylphosphonates, MedChemComm 3 (2012) 65–67.
[27] H.-O. Kalinowski, S. Berger, S. Braun, ^{13}C-NMR-Spektroskopie, Georg Thieme Verlag, Stuttgart, 1984, pp. 530–534.
[28] A. Labed, F. Jiang, I. Labed, A. Lator, M. Peters, M. Achard, A. Kabouche, Z. Kabouche, G.V.M. Sharma, C. Bruneau, Iridium-Catalyzed Sustainable Access to Functionalized Julolidines through Hydrogen Autotransfer, ChemCatChem 7 (7) (2015) 1090–1096.
[29] We thank a reviewer for discussing the possibility of a second order asymmetric induction that may have occurred during the crystallization of **4**. We do not believe that the initially observed solution diastereomer is different than the crystallized diastereomer, in large part because the solvents used are not that polar, and ionization of a metal-oxygen bond seems unlikely.
[30] T.C. Cao, A.L. Cooksy, D.B. Grotjahn, Origins of High Kinetic (*E*)-Selectivity in Alkene Isomerization by a CpRu(PN) Catalyst: a Combined Experimental and Computational Approach, ACS Catal. 10 (2020) 15250–15258, and references therein.